STRAIN LOCALIZATION IN THE BOUNDARY ELEMENT METHOD: THE STRONG DISCONTINUITY APPROACH AS A LIMIT CASE

Rodrigo G. Peixoto

Gabriel O. Ribeiro

Roque L. S. Pitangueira

Samuel S. Penna

rgpeixoto@hotmail.com

gabriel@dees.ufmg.br

roque@dees.ufmg.br

spenna@dees.ufmg.br

Dep. de Eng. de Estruturas, Escola de Engenharia, Universidade Federal de Minas Gerais

Avenida Antônio Carlos, 6627, CEP: 31270-901, Belo Horizonte, MG, Brazil

Abstract. *The Implicit Formulation of the Boundary Element Method (BEM) is used to deal with physically non-linear 2D-problems in solids. An isotropic damage constitutive model, equipped with a strain softening rule, is applied to increasingly narrow bandwidths, determined by mesh refinement, showing the typical post-peak mesh-dependence behaviour. The Continuum Strong Discontinuity Approach (CSDA), characterized by an introduction of discontinuous jumps in the displacement field together with an equilibrium verification (using continuous constitutive models) on the discontinuity line, is also applied to the implicit formulation of the BEM. By a simple numerical example, it is shown that, beyond the mesh independence, the CSDA results represent the limit result of zero localization bandwidth.*

Keywords: *Boundary Element Method, Strain Localization, Continuum Strong Discontinuity Approach*

1 INTRODUCTION

The first developments of boundary integral equations for the treatment of non-linear material behaviour may be attributed to Swedlow and Cruse (1971), Mendelson (1973), Riccardella (1973) and Mukherjee (1977). Later, Bui (1978) presented a corrected way to evaluate derivatives of the singular integrals involving the inelastic fields, introducing new free terms. Those results were then applied to the Boundary Element Method (BEM) by Telles and Brebbia (1979). They used an explicit formulation, where the increment of the initial fields explicitly appears in the non-linear discretized equations and the equilibrium is achieved by a recursive procedure. Considering the proportional relationship between rates of stress and elastic strain, Telles and Carrer (1991) proposed an implicit formulation, where the initial field increments are written in terms of total strain, resulting in an equilibrium matrix equation, which is linearised and incrementally solved. In all above references, elastoplastic constitutive models were considered.

Some material behaviour, e.g., the quasi-brittle ones, requires the introduction of strain softening laws for a correct representation. A direct way to do this is to consider a plasticity model with yield limit degradation, as done by Lin et al. (2002) and Sládek et al. (2003). The presence of strain softening results in a loss of objectiveness with respect to mesh refinements, as the solution tends to an infinitely small localization bandwidth with zero energy dissipation during failure. For that reason, in both works, a non-local procedure, based on the spatial averaging of the plastic multiplier, was also introduced. They differ mainly by the boundary stress evaluation: in the first work, constant functions are used to approximate initial fields inside cells, while, in the second, a regularization of the hypersingular integral equation is adopted. Another non-local plasticity model, based on a re-definition of the yield surface, including a dependency on the Laplacian of the plastic multiplier, was applied to the implicit formulation by Benallal et al. (2002). In that work, a complementary integral representation of the plastic multiplier was discretized and solved together (in a coupled way) to the incremental implicit equation.

An alternative (and perhaps more elegant) way to deal with material's loss of strength, is the adoption of constitutive models based on continuum damage mechanics (CDM). In the BEM context, some works can be cited, such as Rajgelj et al. (1992), Herding and Kuhn (1996), García et al. (1999) and Botta et al. (2005). Specifically, in the last work, the damage model presented by Comi and Perego (2001) was employed. As expected, they also reported mesh dependence when this model is locally applied and an averaging procedure of some strain invariants was introduced, regularizing the model. A more detailed discussion on such localization problems is made by the same authors in a subsequent paper (Benallal et al., 2006).

The Continuum Strong Discontinuity Approach (CSDA), originally introduced by Simo et al. (1993) and later deepened by Oliver (1996), is based on the introduction of discontinuous jumps in the displacement field, which results in unbounded strain values at these points. A continuum constitutive model, equipped with an appropriate softening law, is then applied to characterize the dissipation effects on the discontinuity surface. From the continuity condition of the traction vector across this discontinuity surface, additional equations arrive and are used to evaluate the current displacement jump components. Also, the bounded character of the stress tensor (from its physical sense) leads to a re-interpretation of the hardening-softening modulus of the continuum constitutive model, where the Dirac's delta distribution, associated to an infinitesimally small strain localization band, appears in the new expression. An analysis of the total amount of energy spent for the discontinuity formation, complements such expression introducing, beyond other parameters, the material's fracture energy. This methodology overcomes the mesh dependence associated to strain localization and was applied to the implicit formulation of the BEM by Manzoli and Venturini (2004, 2007) and Manzoli et al. (2009).

In this work, the isotropic damage model developed by Simo and Ju (1987) is used with the implicit formulation of the BEM over finite regions of a specified 2D-domain, under small displacements regime. Strain localization phenomena is verified by taking the dissipation zones of increasingly smaller sizes. The CSDA, using the same constitutive model to represent the discontinuity behaviour, is also worked with the implicit formulation. Little new aspects, such as quadrilateral cells with embedded discontinuity and adoption of the cell's geometry parametrization functions to compose the strong kinematics regularization function, are introduced when comparing to the original works of Manzoli and Venturini (2004, 2007) and Manzoli et al. (2009). In a simple numerical example, results show not only the mesh independence, but also that the CSDA represents the limit situation when the localization bandwidth tends to zero.

The implementations were performed on top of and integrated with the open source software INSANE (INteractive Structural ANalysis Environment), which is available under the GNU General Public License at *http://www.insane.dees.ufmg.br/websvn*.

The paper is divided in more seven sections. In the next section, the integral equations considering initial strain fields and appropriate to deal with standard physically non-linear problems are presented. The numerical counterpart of such equations, re-arranged as required by the implicit formulation, is given in Sec. 3. The CSDA is treated in Secs. 4 and 5, where, respectively, theoretical and numerical aspects are depicted. Section 6 presents the isotropic damage constitutive model adopted and the numerical example worked is described in Sec. 7. Concluding remarks are presented in Sec. 8.

2 STANDARD INTEGRAL EQUATIONS

In quasi-static mechanics of continuous media with small displacements, any point in a non-linear equilibrium path can be defined, independently of the constitutive model, as a combination of two linear parts. Consider, for example, the uni-axial equilibrium paths presented in Fig 1.

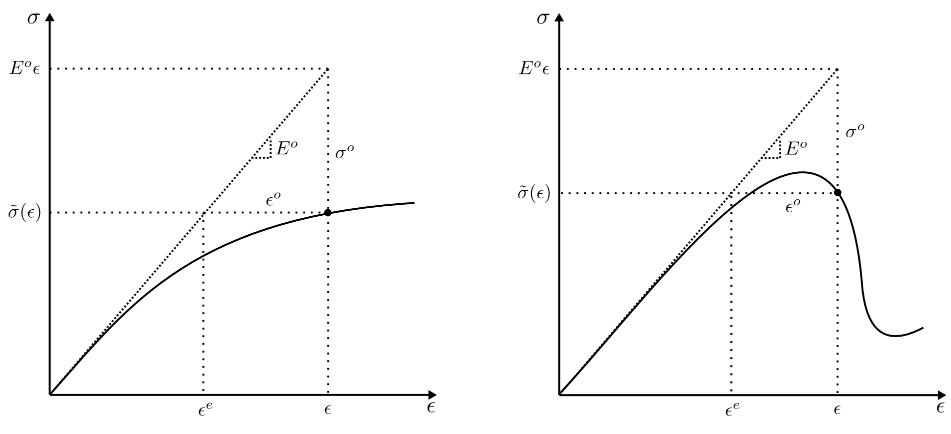

Figure 1: Relations between the stress and strain for two distinct equilibrium paths.

In both cases, for an arbitrary strain state ϵ, the actual stress state which is given by a non-linear constitutive model is represented by $\tilde{\sigma}(\epsilon)$. Additionally, a stress state evaluated using a purely linear elastic relationship for the same arbitrary strain state is given by $E^o\epsilon$, where E^o represents the initial elastic modulus. Also in both cases, the residual quantities ϵ^o and σ^o are defined as the difference between the actual and the purely elastic states. As is possible to note in Fig. 1, and generalizing to a multi-axial solid domain, the total strain ϵ_{ij} and the actual stress $\tilde{\sigma}_{ij}(\epsilon_{ij})$ can be given by

$$\epsilon_{ij} = \epsilon^e_{ij} + \epsilon^o_{ij} \tag{1}$$

$$\tilde{\sigma}_{ij}(\epsilon_{ij}) = E^o_{ijkl}(\epsilon_{kl} - \epsilon^o_{kl}) = E^o_{ijkl}\epsilon_{kl} - \sigma^o_{ij} \tag{2}$$

Thus, the non-linear integral equations in the BEM context are deduced considering the existence of an initial strain field ϵ^o_{ij}, or a corresponding initial stress field $\sigma^o_{ij} = E^o_{ijkl}\epsilon^o_{kl}$, with E^o_{ijkl} representing the linear elastic constitutive tensor. For the first option, the Somigliana's identity for displacements at internal points can be written as

$$\begin{aligned} u_i(\boldsymbol{\xi}) = & \int_\Gamma u^*_{ij}(\boldsymbol{\xi}, \mathbf{X}) t_j(\mathbf{X}) d\Gamma(\mathbf{X}) - \int_\Gamma t^*_{ij}(\boldsymbol{\xi}, \mathbf{X}) u_j(\mathbf{X}) d\Gamma(\mathbf{X}) \\ & + \int_\Omega u^*_{ij}(\boldsymbol{\xi}, \mathbf{X}) b_j(\mathbf{X}) d\Omega(\mathbf{X}) + \int_\Omega \sigma^*_{ijk}(\boldsymbol{\xi}, \mathbf{X}) \epsilon^o_{jk}(\mathbf{X}) d\Omega(\mathbf{X}) \end{aligned} \tag{3}$$

where u_j and t_j represents the displacement and the traction fields at the boundary Γ and b_j are body forces in the domain Ω. The terms u^*_{ij}, t^*_{ij} and σ^*_{ijk} are Kelvin's fundamental solutions, representing respectively, at a field point $\mathbf{X}$, displacements and tractions in direction j and stress components jk due to a unit concentrated force applied at the collocation point $\boldsymbol{\xi}$ acting in direction i. Here, the collocation point is assumed to be internal, i.e., $\{\boldsymbol{\xi} \in \Omega$ and $\boldsymbol{\xi} \notin \Gamma\}$. Expressions for these fundamental solutions are presented in many literature texts, such as Telles (1983), Gao and Davies (2002) and Aliabadi (2002).

If the collocation point is located in domain's boundary, the fundamental solutions' second-order tensors introduce a weakly and a strongly singular character, respectively for the first and second integrals in Eq. (3). Thus, the correct evaluation of the boundary displacement integral equation requires, in this case, a limit process considering a radius of exclusion around the singular point, leading to the following expression:

$$\begin{aligned} c_{ij}(\boldsymbol{\xi}) u_j(\boldsymbol{\xi}) = & \int_\Gamma u^*_{ij}(\boldsymbol{\xi}, \mathbf{X}) t_j(\mathbf{X}) d\Gamma(\mathbf{X}) - \fint_\Gamma t^*_{ij}(\boldsymbol{\xi}, \mathbf{X}) u_j(\mathbf{X}) d\Gamma(\mathbf{X}) \\ & + \int_\Omega u^*_{ij}(\boldsymbol{\xi}, \mathbf{X}) b_j(\mathbf{X}) d\Omega(\mathbf{X}) + \int_\Omega \sigma^*_{ijk}(\boldsymbol{\xi}, \mathbf{X}) \epsilon^o_{jk}(\mathbf{X}) d\Omega(\mathbf{X}) \end{aligned} \tag{4}$$

where $c_{ij}(\boldsymbol{\xi})$ is a function of the boundary's geometry around the collocation point and the elastic properties of the material. It is also important to emphasize that the second integral exists only in the Cauchy's Principal Value (CPV) sense, as indicated by the crossed integral symbol.

Furthermore, internal strains can be obtained by taking the symmetric part of the gradient of Eq. (3), related to the collocation point, resulting in

$$\begin{aligned}\epsilon_{ij}(\boldsymbol{\xi}) = &\int_{\Gamma} u^*_{ijk}(\boldsymbol{\xi}, \mathbf{X}) t_k(\mathbf{X}) d\Gamma(\mathbf{X}) - \int_{\Gamma} t^*_{ijk}(\boldsymbol{\xi}, \mathbf{X}) u_k(\mathbf{X}) d\Gamma(\mathbf{X}) \\ &+ \int_{\Omega} u^*_{ijk}(\boldsymbol{\xi}, \mathbf{X}) b_k(\mathbf{X}) d\Gamma(\mathbf{X}) + \fint_{\Omega} \sigma^*_{ijkl}(\boldsymbol{\xi}, \mathbf{X}) \epsilon^o_{kl}(\mathbf{X}) d\Omega(\mathbf{X}) \\ &+ F^{\epsilon\epsilon}_{ijkl} \epsilon^o_{kl}(\boldsymbol{\xi})\end{aligned} \tag{5}$$

where the last domain integral have a strongly singular kernel when the collocation and field points coincide and, again, its evaluation exists only in the CPV sense. Tensors u^*_{ijk}, t^*_{ijk} and σ^*_{ijkl} are respectively obtained by taking the gradients of fundamental solutions u^*_{ij}, t^*_{ij} and σ^*_{ijk}, while $F^{\epsilon\epsilon}_{ijkl}$ is the free term, which existence was firstly verified by Bui (1978).

3 NON-LINEAR IMPLICIT FORMULATION OF THE BEM

Absence of body forces will be considered from now on. Taking the discretization of domain's boundary and the part of the domain where initial fields are present, as usual in the BEM, Eq. (4) assumes the following form after its application to all boundary collocation points and re-arrangement of boundary prescribed conditions in the same vector:

$$[A]\{x\} = [B]\{y\} + [Q_{\epsilon^o}]\{\epsilon^o\} \tag{6}$$

where $\{x\}$ and $\{y\}$ are, respectively, the boundary unknowns and prescribed displacement or traction components, $\{\epsilon^o\}$ represents the initial strain components and matrices $[A]$, $[B]$ and $[Q_{\epsilon^o}]$ hold the integration coefficients.

Also, by applying Eq. (5) to all internal collocation points, a matrix equation can be written as

$$\{\epsilon\} = [A^\epsilon]\{x\} + [B^\epsilon]\{y\} + [Q^\epsilon_{\epsilon^o}]\{\epsilon^o\} \tag{7}$$

where $\{\epsilon\}$ represents a vector with internal collocation points strain components and matrices $[A^\epsilon]$, $[B^\epsilon]$ and $[Q^\epsilon_{\epsilon^o}]$ are also assembled with integration coefficients.

The Implicit Formulation of the BEM begins by solving Eq. (6) for $\{x\}$, i.e.,

$$\{x\} = [N]\{y\} + [M_{\epsilon^o}]\{\epsilon^o\} \tag{8}$$

where

$$\begin{aligned}[N] &= [A^{-1}][B] \\ [M_{\epsilon^o}] &= [A^{-1}][Q_{\epsilon^o}]\end{aligned} \tag{9}$$

Then, by applying Eq. (8) to Eq. (7), the following result is obtained:

$$\{\epsilon\} = [N^\epsilon]\{y\} + [M^\epsilon_{\epsilon^o}]\{\epsilon^o\} \tag{10}$$

where

$$
\begin{aligned}
&[N^{\epsilon}] = [A^{\epsilon}][A^{-1}][B] + [B^{\epsilon}] \\
&[M^{\epsilon}_{\epsilon^o}] = [A^{\epsilon}][A^{-1}][Q_{\epsilon^o}] + [Q^{\epsilon}_{\epsilon^o}]
\end{aligned}
\tag{11}
$$

Taking Eq. (2) into account, Eq. (10) is clearly non-linear, requiring incremental-iterative procedures for its evaluation. Thus, considering the *i*-th increment of the prescribed loads $\{y\}$, this equation is rewritten as

$$
\{\epsilon\}^i = \lambda^i[N^{\epsilon}]\{y\} + [M^{\epsilon}_{\epsilon^o}]\{\epsilon^o\}^i \tag{12}
$$

where the load factor λ^i is a cumulative scalar quantity which defines the external load increment. Its value is defined by the control method employed.

From Eq. (12), an equilibrium condition vector $\{Q\}^i$ can be defined with the introduction of the matrix form of Eq. (2), i.e.,

$$
\{Q\}^i = \lambda^i[N^{\epsilon}]\{y\} + [M^{\epsilon}_{\epsilon^o}]\big(\{\epsilon\}^i - [E^o]^{-1}\{\tilde{\sigma}(\epsilon)\}^i\big) - \{\epsilon\}^i = \{0\} \tag{13}
$$

where $[E^o]$ is a quasi-diagonal matrix representing the linear elastic constitutive relationship and $\{\tilde{\sigma}(\epsilon)\}$ is the appropriate stress vector, corresponding to the strain state, in the constitutive model chosen.

Now, by considering the *j*-th Newton's iteration within the *i*-th increment, an additive correction can be defined as

$$
\delta()^i_j = ()^i_j - ()^i_{j-1} \tag{14}
$$

and Eq. (13) is conveniently rewritten as

$$
\{Q\}^i_j = \lambda^i_j[N^{\epsilon}]\{y\} + [M^{\epsilon}_{\epsilon^o}]\big(\{\epsilon\}^i_j - [E^o]^{-1}\{\tilde{\sigma}(\epsilon)\}^i_j\big) - \{\epsilon\}^i_j = \{0\} \tag{15}
$$

Solutions for Eq. (13) are essentially the Implicit BEM Formulation introduced by Telles and Carrer (1991). In this work a solution strategy that permits de usage of different control methods and an unified constitutive modelling framework, described in Anacleto et al. (2013), was adopted.

3.1 Integrals treatment

The regular integrals in Eqs. (4) and (5) are solved by conventional Gaussian quadrature. The boundary and domain weakly singular integrals, involving the kernels containing u^*_{ij} and σ^*_{ijk}, are solved using the methods presented respectively in Huang and Cruse (1993) and Lachat and Watson (1976). For evaluation of the boundary strongly singular integral in Eq. (4), the methodology described in Guiggiani and Casalini (1987) was employed, while for the domain strongly singular integral of Eq. (5), the procedure from Gao and Davies (2000) was adopted.

The initial strain field was approximated by constant values inside internal cells, in such a way that boundary recovery techniques or hyper-singular integrals evaluations were avoided.

4 THE CONTINUUM STRONG DISCONTINUITY APPROACH

Theoretical remarks of the CSDA are presented in this section. Only the essential features, necessary to a well understanding of this paper scope, are presented. A more complete description of the strong discontinuity analysis can be found in Oliver (1996).

4.1 Strong Discontinuity Kinematics

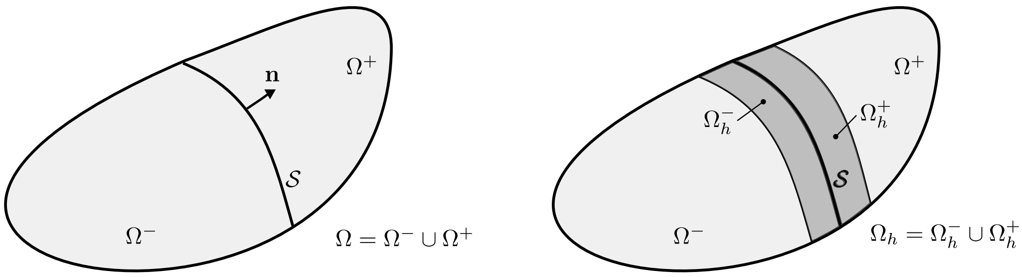

(a) (b)

Figure 2: Solid with discontinuity surface

Referring to Fig. 2a, the displacement vector field can be written as

$$u_i(\mathbf{X},t) = \bar{u}_i(\mathbf{X},t) + \mathcal{H}_{\mathcal{S}}(\mathbf{X})[\![u_i]\!](\mathbf{X},t) \tag{16}$$

where $\bar{u}_i(\mathbf{X},t)$ is the regular part of the displacement field and $[\![u_i]\!](\mathbf{X},t)$ are continuous functions over the solid domain that represent the displacement jump in the discontinuity surface $\mathcal{S}$, supported by the Heaviside function $\mathcal{H}_{\mathcal{S}}(\mathbf{X})$ ($\mathcal{H}_{\mathcal{S}} = 1\ \forall \mathbf{X} \in \Omega^+$ and $\mathcal{H}_{\mathcal{S}} = 0\ \forall \mathbf{X} \in \Omega^-$).

As usual, the corresponding strain field can be obtained from Eq. (16) by taking the symmetric part of the gradient in such a way that

$$\begin{aligned}\epsilon_{ij} &= \underbrace{\frac{1}{2}(\bar{u}_{i,j} + \bar{u}_{j,i}) + \frac{\mathcal{H}_{\mathcal{S}}}{2}([\![u_{i,j}]\!] + [\![u_{j,i}]\!])}_{\bar{\epsilon}_{ij}} + \frac{\delta_{\mathcal{S}}}{2}([\![u_i]\!]n_j + [\![u_j]\!]n_i) \\ &= \bar{\epsilon}_{ij} + \frac{\delta_{\mathcal{S}}}{2}([\![u_i]\!]n_j + [\![u_j]\!]n_i)\end{aligned} \tag{17}$$

where $\bar{\epsilon}_{ij}$ is the regular part of the strain field exhibiting, at most, bounded discontinuities across $\mathcal{S}$, while $\delta_{\mathcal{S}}$ is the Dirac's line delta-function over $\mathcal{S}$. The components n_i refer to the unitary vector, normal to the discontinuity surface.

As detailed by Oliver (1996), the imposition of essential boundary conditions cannot be done just on one of the fields $\bar{u}_i$ or $[\![u_i]\!]$, and a reformulation of the kinematics needs to be performed. Such reformulation begins with the assumption of an additional arbitrary sub-domain $\Omega_h \subset \Omega$ surrounding $\mathcal{S}$ as presented in Fig. 2b. It is assumed that the boundary Γ_u, where the essential boundary conditions are imposed, is outside Ω_h ($\Gamma_u \cap \Omega_h = \emptyset$).

Then, one can define a continuous function $\varphi(\mathbf{X})$ which is completely arbitrary except for the following two conditions:

$$\begin{aligned}\varphi(\mathbf{X}) &= 0, \forall \mathbf{X} \in \Omega^- \backslash \Omega_h^- \\ \varphi(\mathbf{X}) &= 1, \forall \mathbf{X} \in \Omega^+ \backslash \Omega_h^+\end{aligned} \tag{18}$$

where $a\backslash b$ means a excluding b.

Equation (16) can now be rewritten as

$$\begin{aligned} u_i(\mathbf{X},t) &= \underbrace{\bar{u}_i(\mathbf{X},t) + \varphi(\mathbf{X})[\![u_i]\!](\mathbf{X},t)}_{\hat{u}_i(\mathbf{X},t)} + \underbrace{\left[\mathcal{H}_{\mathcal{S}}(\mathbf{X}) - \varphi(\mathbf{X})\right]}_{\mathcal{M}^h_{\mathcal{S}}(\mathbf{X})}[\![u_i]\!](\mathbf{X},t) \\ &= \hat{u}_i(\mathbf{X},t) + \mathcal{M}^h_{\mathcal{S}}(\mathbf{X})[\![u_i]\!](\mathbf{X},t) \end{aligned} \tag{19}$$

where $\hat{u}_i(\mathbf{X},t)$ are continuous functions and $\mathcal{M}^h_{\mathcal{S}}(\mathbf{X})$ takes zero value everywhere in Ω, except in Ω_h.

Hence, the kinematic description of the displacement field is made now, according to Eq. (19), in terms of the regular part $\hat{u}(\mathbf{X},t)$ plus the term $\mathcal{M}^h_{\mathcal{S}}(\mathbf{X})[\![u_i]\!](\mathbf{X},t)$, which contains the jump and whose support is Ω_h. Thus, the essential boundary conditions can be applied exclusively on the term $\hat{u}(\mathbf{X},t)$.

Now, taking the symmetric part of the gradient of Eq. (19), the total strain field assumes the form

$$\begin{aligned} \epsilon_{ij} &= \frac{1}{2}(\hat{u}_{i,j} + \hat{u}_{j,i}) + \underbrace{\frac{\mathcal{M}^h_{\mathcal{S}}}{2}([\![u_{i,j}]\!] + [\![u_{j,i}]\!]) - \frac{1}{2}(\varphi_{,i}[\![u_j]\!] + \varphi_{,j}[\![u_i]\!])}_{-\epsilon^{\varphi}_{ij}} + \frac{\delta_{\mathcal{S}}}{2}([\![u_i]\!]n_j + [\![u_j]\!]n_i) \\ &= \hat{\epsilon}_{ij} - \epsilon^{\varphi}_{ij} + \frac{\delta_{\mathcal{S}}}{2}([\![u_i]\!]n_j + [\![u_j]\!]n_i) \end{aligned} \tag{20}$$

where $\hat{\epsilon}_{ij}$ is a regular part, ϵ^{φ}_{ij} have non-zero values only inside the sub-domain Ω_h and the last term is limited to the discontinuity line $\mathcal{S}$.

4.2 Discontinuity interface equilibrium

In the CSDA, an appropriate (continuum) constitutive model is used to describe the dissipation process on points over the discontinuity surface $\mathcal{S}$. The constitutive equation, relating stress to the total strain, of a such model is generically represented here by

$$\sigma^{\mathcal{S}}_{ij}(\epsilon_{ij}) \equiv \sigma^{\mathcal{S}}_{ij}(\hat{\epsilon}_{ij}, [\![u_i]\!], [\![u_{i,j}]\!]) \tag{21}$$

where ϵ_{ij} is given by Eq. (20) and the dependence on $\varphi(\mathbf{X})$ and n_i were avoided by the arbitrariness of the first and by considering the material character of the discontinuity, i.e., once initiated, its orientation remains fixed.

Domain points outside of $\mathcal{S}$ are considered in this work to stay in a linear elastic regime. Thus, the constitutive relation for these points can be written as

$$\sigma^{\Omega\backslash\mathcal{S}}_{ij}(\epsilon_{ij}) = E^o_{ijkl}\epsilon_{kl} = E^o_{ijkl}\left[\hat{\epsilon}_{kl} - \epsilon^{\varphi}_{kl}([\![u_i]\!], [\![u_{i,j}]\!])\right] \tag{22}$$

The equilibrium condition requires continuity of the traction vector on $\mathcal{S}$, i.e.,

$$\sigma^{\Omega\backslash\mathcal{S}}_{ij}n_j = \sigma^{\mathcal{S}}_{ij}n_j \tag{23}$$

or, by applying Eqs. (21) and (22),

$$f_i = \left[E^o_{ijkl}\left[\hat{\epsilon}_{kl} - \epsilon^{\varphi}_{kl}([\![u_i]\!], [\![u_{i,j}]\!])\right] - \sigma^{\mathcal{S}}_{ij}(\epsilon_{ij})\right]n_j = 0 \tag{24}$$

4.3 Regularized constitutive model

In the BEM context, the numerical solution of Eq. (24) is made by adoption of internal cells with embedded discontinuity and furnishes the displacement jump components, $[\![u_i]\!]$, required for the evaluation of ϵ_{ij}^{φ}. As will be clear in Sec. 5, these jump components are considered constants inside a cell, resulting in a null gradient tensor. Thus, for a given $\hat{\epsilon}_{ij}$ and considering Eq. (20) , Eq. (24) has as only unknown variables the components $[\![u_i]\!]$, i.e., $f_i \equiv f_i([\![u_i]\!]) = 0$.

A regularized constitutive model, relating stress to regular strain ($\hat{\epsilon}_{ij}$), can then be defined from Eq. (22):

$$\tilde{\sigma}_{ij}(\hat{\epsilon}_{ij}) = \sigma_{ij}^{\Omega\backslash\mathcal{S}}\left(\hat{\epsilon}_{ij} - \epsilon_{ij}^{\varphi}\big([\![u_i]\!](\hat{\epsilon}_{ij})\big)\right) = E_{ijkl}^{o}(\hat{\epsilon}_{kl} - \epsilon_{kl}^{\varphi}) \tag{25}$$

where $[\![u_i]\!](\hat{\epsilon}_{ij})$ represents the solution of Eq. (24).

5 NUMERICAL ASPECTS

From the similarities between Eqs. (2) and (25), integral equations concerning discontinuity surfaces in the domain can be obtained, resulting in expressions of the same forms as presented in Sec. 2, considering only the substitution of terms depicted in Table 1. A more formal demonstration can be found in Manzoli and Venturini (2004).

Table 1: Correspondent terms for integral equations

Standard Integral Equations	IE with discontinuity surface
u_i	$\hat{u}_i$
ϵ_{ij}	$\hat{\epsilon}_{ij}$
ϵ_{ij}^{o}	ϵ_{ij}^{φ}

For that reason, the numerical treatment detailed in Sec. 3 can also be used for problems involving strong discontinuities, if the regularized constitutive model is employed. Additional numerical aspects regarding internal cells with embedded discontinuity, evaluation of displacement jumps and the regularized constitutive model tangent operator are presented next.

5.1 Cells with embedded discontinuity

From conditions of Eq. (18), strong discontinuity dissipative effects are restricted to the sub-domain Ω_h, defined in Fig. 2b, and only this region needs to be discretized by cells, as illustrated in Fig. 3a.

For each internal cell with embedded discontinuity, typically represented in Fig. 3b, only one collocation point is adopted and the field ϵ_{ij}^{φ} is considered constant inside the entire cell domain, i.e., for $\mathbf{X} \in \Omega_c$,

$$\begin{Bmatrix} \epsilon_{11}^{\varphi}(\mathbf{X}) \\ \epsilon_{22}^{\varphi}(\mathbf{X}) \\ \epsilon_{12}^{\varphi}(\mathbf{X}) \end{Bmatrix} \approx \begin{Bmatrix} \epsilon_{11}^{\varphi,c} \\ \epsilon_{22}^{\varphi,c} \\ \epsilon_{12}^{\varphi,c} \end{Bmatrix} = \{\epsilon^{\varphi,c}\} \tag{26}$$

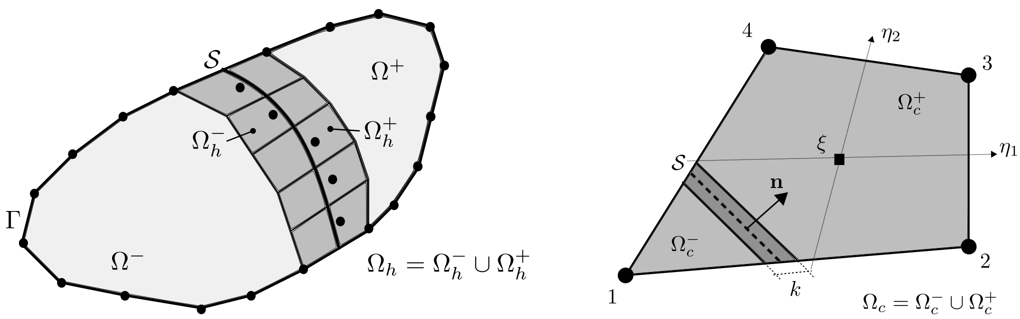

(a) Boundary and domain discretization (b) Cell with embedded discontinuity

Figure 3: BEM discretization of a solid with discontinuity surface

However, the geometry of each cell is parametrized by conventional linear shape functions defined by natural coordinates η_i, i.e.,

$$X_j(\eta_1, \eta_2) \approx M^{\alpha}(\eta_1, \eta_2) X_j^{\alpha} \tag{27}$$

where index α refer to vertices points (numbered from 1 to 4 in Fig. 3b).

Thus, in a cell with embedded discontinuity, one can distinguish an internal collocation point and a set of geometric interpolation points. Other important attributes are the orientation of the discontinuity line (given by its normal vector) and a small valued parameter, k, used for the regularization of the Dirac's delta distribution.

The geometric interpolation functions can also be used to define the function $\varphi(\mathbf{X})$ inside the cell, since the conditions of Eq. (18) are fulfilled by the choice:

$$\varphi(\mathbf{X}(\eta_1, \eta_2)) = \sum_{\alpha^+} M^{\alpha^+}(\eta_1, \eta_2) \tag{28}$$

where the summation is taken over the interpolation functions associated to the geometric vertices located at Ω_c^+ side of the cell. For example, in Fig. 3b, $\alpha^+ = 2, 3, 4$.

5.2 Evaluation of displacement jumps

The displacement jump inside a cell with embedded discontinuity is obtained from the numerical solution of Eq. (24), i.e., the interface equilibrium equation. To do this, more two assumptions need to be made. The first one is to consider the functions $[\![u_i]\!](\mathbf{X})$ as constants inside the cell domain, i.e.,

$$\begin{cases} [\![u_i]\!](\mathbf{X}) \approx \left\{ [\![u_1]\!] \quad [\![u_2]\!] \right\}^T = \{[\![u]\!]\} & \text{for} \quad \mathbf{X} \in \Omega_c \\ [\![u_{i,j}]\!](\mathbf{X}) = 0 & \text{for} \quad \mathbf{X} \in \Omega_c \end{cases} \tag{29}$$

The second assumption is the regularization of of the Dirac's delta distribution by the small valued parameter k, i.e.,

$$\begin{cases} \delta_{\mathcal{S}} \approx \dfrac{1}{k} & \text{for} \quad \mathbf{X} \in \mathcal{S} \\ \delta_{\mathcal{S}} = 0 & \text{for} \quad \mathbf{X} \in \Omega \backslash \mathcal{S} \end{cases} \tag{30}$$

Using Eqs. (29) and (30), the vector of Eq. (26) can be written in terms of the displacement jump:

$$\{\epsilon^{\varphi,c}\} = \begin{Bmatrix} \epsilon_{11}^{\varphi,c} \\ \epsilon_{22}^{\varphi,c} \\ \epsilon_{12}^{\varphi,c} \end{Bmatrix} = \begin{bmatrix} \varphi_{,1} & 0 \\ 0 & \varphi_{,2} \\ \frac{1}{2}\varphi_{,2} & \frac{1}{2}\varphi_{,1} \end{bmatrix} \begin{Bmatrix} [\![u_1]\!] \\ [\![u_2]\!] \end{Bmatrix} = [\nabla\varphi]\{[\![u]\!]\} \tag{31}$$

where, from Eqs. (27) and (28),

$$\varphi_{,i} = \frac{\partial\varphi}{\partial\eta_k}\frac{\partial\eta_k}{\partial X_i} = \left(\frac{\partial M^\alpha}{\partial\eta_k}X_i^\alpha\right)^{-1}\frac{\partial\varphi}{\partial\eta_k} = \left(\frac{\partial M^\alpha}{\partial\eta_k}X_i^\alpha\right)^{-1}\left(\frac{\partial}{\partial\eta_k}\left[\sum_{\alpha^+} M^{\alpha^+}\right]\right) \tag{32}$$

Thus, using Eqs. (30) and (31), the following matrix form of Eq. (24) is obtained:

$$\{f\} = [\bar{N}^c]^T\big([E^o]\{\hat{\epsilon}^c\} - [E^o][\nabla\varphi]\{[\![u]\!]\} - \{\sigma^{\mathcal{S}}(\{\hat{\epsilon}^c\} - [\nabla\varphi]\{[\![u]\!]\} + \frac{1}{k}[N^c]\{[\![u]\!]\})\}\big) = \{0\} \tag{33}$$

where,

$$[\bar{N}^c] = \begin{bmatrix} n_1 & 0 & n_2 \\ 0 & n_2 & n_1 \end{bmatrix}^T ; \qquad [N^c] = \begin{bmatrix} n_1 & 0 & \frac{1}{2}n_2 \\ 0 & n_2 & \frac{1}{2}n_1 \end{bmatrix}^T \tag{34}$$

Finally, Eq. (33) is solved by Newton's iterative method, noting that its linearised form, for a known $\{\hat{\epsilon}^c\}$, is given by

$$\{f\}_{j-1} + \frac{\partial\{f\}_{j-1}}{\partial\{[\![u]\!]\}_{j-1}}\{\delta[\![u]\!]\}_j \approx \{0\} \tag{35}$$

where,

$$\left[\frac{\partial\{f\}}{\partial\{[\![u]\!]\}}\right]_{j-1} = [\bar{N}^c]^T\left[-[E^o][\nabla\varphi] - \left[\frac{\partial\sigma^{\mathcal{S}}}{\partial\epsilon}\right]_{j-1}\left[\frac{1}{k}[N^c] - [\nabla\varphi]\right]\right] \tag{36}$$

5.3 Regularized constitutive model

The matrix form of the regularized constitutive model, Eq. (25), for an internal cell is given by

$$\{\tilde{\sigma}(\hat{\epsilon}^c)\} = [E^o](\{\hat{\epsilon}^c\} - [\nabla\varphi]\{[\![u]\!]\}) = [E^o](\{\hat{\epsilon}^c\} - \{\epsilon^{\varphi,c}\}) \tag{37}$$

Also, the tangent operator associated to this regularized constitutive model and necessary for the solution of implicit BEM formulation's equilibrium condition vector of Eq. (13), can be obtained from Eq. (37), i.e,

$$\left[\frac{\partial\tilde{\sigma}}{\partial\hat{\epsilon}^c}\right] = [E^o]\left([I] - [\nabla\varphi]\left[\frac{\partial\{f\}}{\partial\{[\![u]\!]\}}\right]^{-1}[\bar{N}^c]^T\left([E^o] - \left[\frac{\partial\sigma^{\mathcal{S}}}{\partial\epsilon}\right]\right)\right) \tag{38}$$

6 ISOTROPIC DAMAGE CONSTITUTIVE MODEL

The isotropic damage (continuum) constitutive model proposed by Simo and Ju (1987) is used in this work to represent damage dissipation in finite regions of a solid domain and the discontinuity line behaviour in the CSDA. Such constitutive model can be briefly stated by the next expressions:

$$\text{Constitutive equation:} \quad \sigma_{ij} = (1-D)E^{o}_{ijkl}\epsilon_{kl} = E_{ijkl}\epsilon_{kl}; \tag{39a}$$

$$\text{Damage variable:} \quad D \equiv D(r) = 1 - \frac{q(r)}{r}, \quad D \in [0,1]; \tag{39b}$$

$$\text{Internal variable evolution law:} \quad \dot{r} = \dot{\lambda}, \quad \begin{cases} r \in [r_o, \infty), \\ r_o = r|_{t=0} = \frac{f_t}{\sqrt{E}}; \end{cases} \tag{39c}$$

$$\text{Damage criterion:} \quad \begin{cases} F(\sigma_{ij}, q) \equiv \tau_\sigma - q = \sqrt{\sigma_{ij} E^{o,-1}_{ijkl} \sigma_{kl}} - q \quad \text{(stress space)} \\ \text{or} \\ \bar{F}(\epsilon_{ij}, r) \equiv \tau_\epsilon - r = \sqrt{\epsilon_{ij} E^{o}_{ijkl} \epsilon_{kl}} - r \quad \text{(strain space);} \end{cases} \tag{39d}$$

$$\text{Loading-unloading conditions:} \quad F \leqslant 0, \quad \dot{\lambda} \geqslant 0, \quad \dot{\lambda} F = 0, \quad \dot{\lambda}\dot{F} = 0 \tag{39e}$$

$$\text{Hardening rule:} \quad \dot{q} = H(r)\dot{r}, \quad (H = q'(r) \leqslant 0), \quad \begin{cases} q \in [0, r_o], \\ q|_{t=0} = r_o \end{cases} \tag{39f}$$

where σ_{ij} in Eq. (39a) represents directly the actual stress $\tilde{\sigma}_{ij}$, from Eq. (2), for finite bands with damage or σ^{S}_{ij}, from Eq. (21), for the CSDA, $E_{ijkl} = (1-D)E^{o}_{ijkl}$ is the secant constitutive tensor, q is the stress-like internal variable, while r is the strain-like internal variable. The value r_o is the threshold that determines the initial elastic domain, which can be characterized in terms of the uniaxial elastic strength f_t and the elastic modulus E - see Eq. (39c).

A tangent counterpart of the relation presented in Eq. 39a can be written as

$$\dot{\sigma}_{ij} = E^{t}_{ijkl}\dot{\epsilon}_{kl}; \quad E^{t}_{ijkl} = E_{ijkl} + \frac{1}{\bar{H}}\bar{m}_{ij}\bar{n}_{kl} \tag{40}$$

where

$$\frac{1}{\bar{H}} = \frac{\partial D}{\partial r} = \frac{q}{r^2} - \frac{H}{r} \tag{41}$$

$$\bar{n}_{ij} = \frac{\partial \bar{F}}{\partial \epsilon_{ij}} = \frac{1}{\tau_\epsilon} E^{o}_{ijkl}\epsilon_{kl} \tag{42}$$

$$\bar{m}_{ij} = -E^{o}_{ijkl}\epsilon_{kl} \tag{43}$$

An exponential damage law compatible with the strong discontinuity regime, according to Manzoli et al. (2009), was employed in this work for both cases: damage in finite regions and the strong discontinuity approach. Such expression is given by

$$D(r) = 1 - \frac{r_o}{r} e^{(1-\frac{r}{r_o})\frac{r_o^2}{G_f}k} \tag{44}$$

where G_f is the fracture energy and k is the same regularization parameter for Dirac's delta function distribution used to state the discontinuity interface equilibrium condition.

7 NUMERICAL EXAMPLE

A simple traction example, with geometry, material properties, boundary conditions and loads presented in Fig. 4, is analysed here.

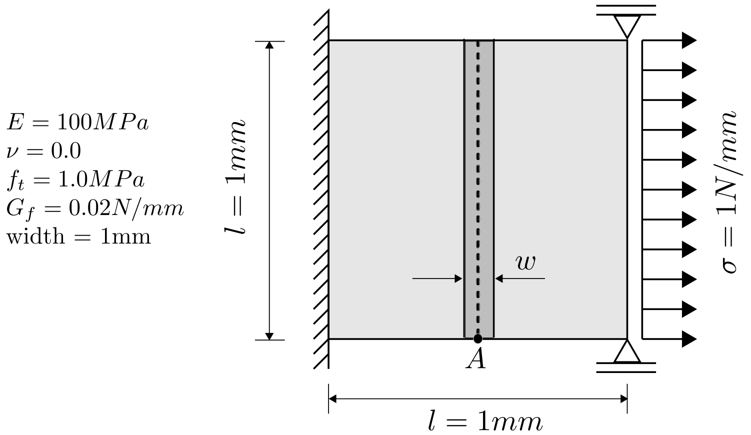

Figure 4: Simple traction example; problem statement

Three different meshes, as shown in Fig. 5, are used to represent increasingly narrow bandwidths of strain localization, where the continuum isotropic damage constitutive model is applied without any introduction of discontinuities in the displacement field. Constant approximation of the initial strains, ϵ^o_{ij}, is considered inside the internal cells. The same meshes are re-analysed with the CSDA, by the application of cells with embedded strong discontinuity. Linear boundary elements were employed in both cases. Also, for Eq. (44), $k = 0.01mm$ was adopted.

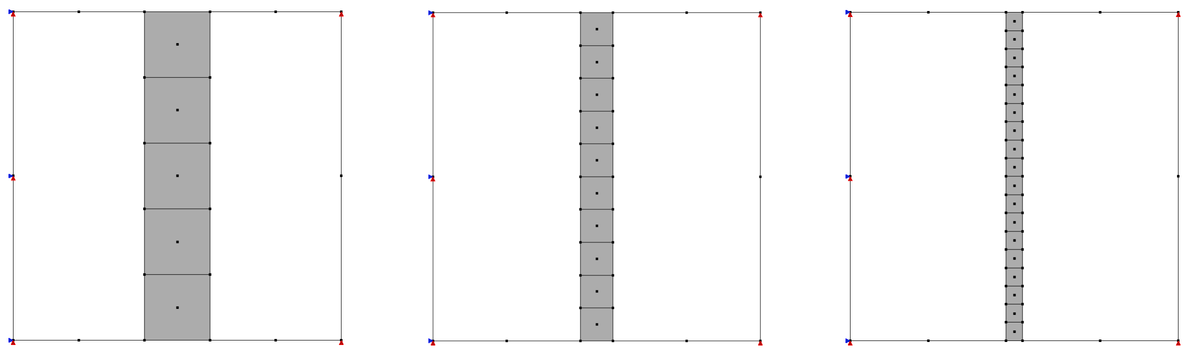

(a) Mesh 01 (w = 0.20mm) (b) Mesh 02 (w = 0.10mm) (c) Mesh 03 (w = 0.05mm)

Figure 5: Simple traction example; meshes

Actually, for the CSDA analysis, a propagation algorithm was used, where a cell is activated as the elastic limit is firstly exceeded in an adjacent cell. Thus, it is only necessary to previously specify the discontinuity's beginning point (represented by point A in Fig. 4). The discontinuity line orientation inside the cell is obtained by taking its normal parallel to the first principal stress direction at its initiation time. Some results are presented in Fig. 6.

In Fig. 6a, an equilibrium path, represented by the cumulative load factor in function of the loaded edge displacement is presented for the three meshes. Mesh independence is observed, as expected for the CSDA. The displacement jump effect is shown in Fig. 6b, where the longitudinal displacements along the lower edge, after 20% of the analysis, are plotted.

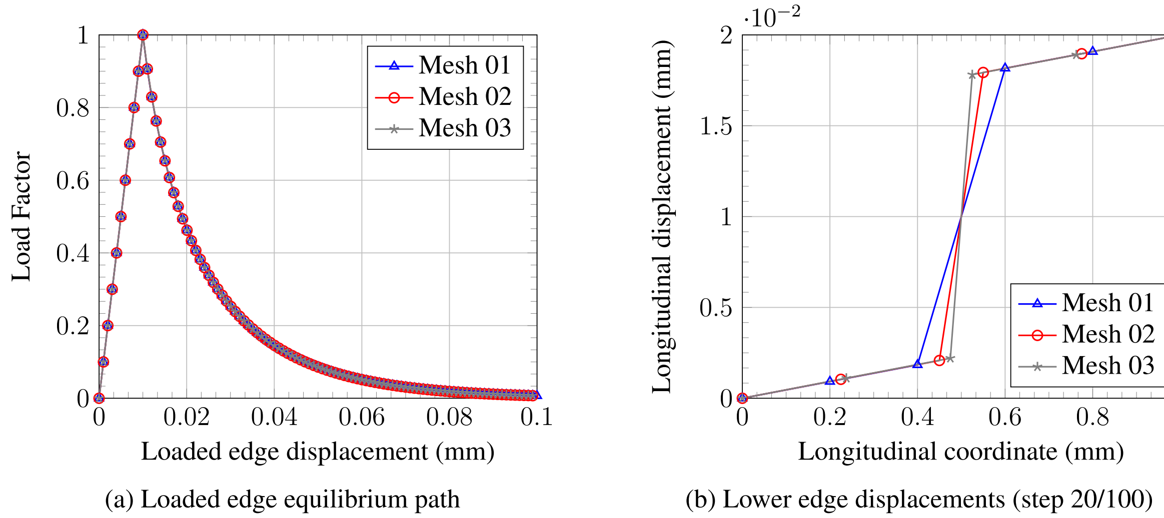

Figure 6: Results for simple traction example with strong discontinuity approach.

The equilibrium paths obtained for the continuum case are presented in Fig. 7. The mesh dependence for the post-peak behaviour is verified, with more accentuated decreasing curves as small is the localization bandwidth.

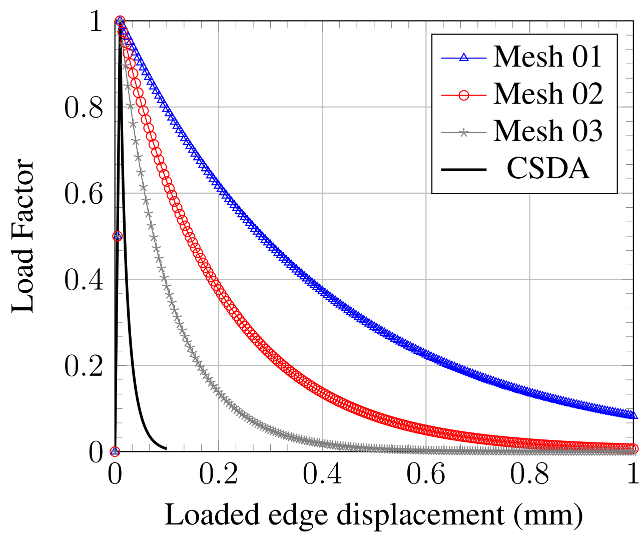

Figure 7: Results for simple traction example with continuum constitutive model.

The CSDA results are also re-plotted in Fig. 7, showing that they represent the limit case of a zero width localization band if the same continuum constitutive model is used in finite regions of the domain and to represent the discontinuity behaviour.

8 CONCLUDING REMARKS

The implicit formulation of the BEM was applied for solution of two dimensional solid mechanics non-linear problems. For material behaviour, an isotropic damage constitutive model, with an exponential damage evolution law, was considered. Strain localization phenomena was addressed by confining the dissipative effects to increasingly narrow bandwidths. As expected, for a smaller localization bandwidth, a faster strength reduction was observed. For that reason, the treatment of discontinuities in the kinematic fields by continuum constitutive models, frequently requires the adoption of a regularizing technique.

Then, the CSDA, which consists in the application of discontinuous displacement fields to continuum constitutive models (compatible with the condition of traction continuity across the discontinuous surface), was also applied to implicit BEM formulation, following the ideas of Manzoli and Venturini (2004, 2007) and Manzoli et al. (2009). For the authors' knowledge, these are the only works available in literature that deals with CSDA together with the BEM. In this sense, the present work brings some little innovative aspects such as:

i. usage of quadrilateral internal cells with embedded discontinuity;

ii. adoption of the cell's geometry parametrization (shape) functions to construct the kinematics regularizing function $\varphi(\mathbf{X})$ - see Eq. (28) - in a similar way as done in Finite Element Method treatment of the CSDA (e.g., Oliver (1996)).

The results obtained with the CSDA showed mesh independence behaviour and, as predicted by the theory, correspond to the limit situation of inelastic strain localization, when the localization bandwidth tends to zero.

ACKNOWLEDGEMENTS

The authors gratefully acknowledge the important support of the Brazilian research agencies FAPEMIG (in Portuguese "Fundação de Amparo à Pesquisa do Estado de Minas Gerais" - Grants PPM-00669-15 and PPM-00307-13), CNPq (in Portuguese "Conselho Nacional de Desenvolvimento Cintífico e Tecnológico" - Grants 308785/2014-2 and 311109/2013-6).

REFERENCES

Aliabadi, M. H., 2002. *The Boundary Element Method - Volume 2: Applications in Solids and Structures*. John Wiley & Sons.

Anacleto, F., Peixoto, R., Penna, S., Ribeiro, G., Pitangueira, R., & Ribeiro, T., 2013. Nonlinear solution algorithm for the implicit boundary element method concerning various control methods. In Del Prado, Z. J. G. N., ed, *Proceedings of the XXXIV Iberian Latin-American Congress on Computational Methods in Engineering (CILAMCE 2013)*.

Benallal, A., Botta, A. S., & Venturini, W. S., 2006. On the description of localization and failure phenomena by the boundary element method. *Computer Methods in Applied Mechanics and Engineering*, vol. 195, pp. 5833-5856.

Benallal, A., Fudoli, C. A., & Venturini, W. S., 2002. An implicit BEM formulation for gradient plasticity and localization phenomena. *International Journal for Numerical Methods in Engineering*, vol. 53, pp. 1853-1869.

Botta, A. S., Venturini, W. S., & Benallal, A., 2005. BEM applied to damage models emphasizing localization and associated regularization techniques. *Engineering Analysis with Boundary Elements*, vol. 29, pp. 814-827.

Bui, H. D., 1978. Some remarks about the formulation of three-dimensional thermoelastoplastic problems by integral equations. *International Journal of Solids and Structures*, vol. 14, pp. 935-939.

Comi, C., & Perego, U., 2001. Fracture energy based bi-dissipative damage model for concrete. *International Journal of Solids and Structures*, vol. 38, pp. 6427-6454.

Gao, X.-W., & Davies, T. G., 2000. An effective boundary element algorithm for 2D and 3D elastoplastic problems. *International Journal of Solids and Structures*, vol. 37, pp. 4987-5008.

Gao, X.-W., & Davies, T. G., 2002. *Boundary Element Programming in Mechanics*. Cambridge University Press.

García, R., Flórez-López, J., & Cerrolaza, M., 1999. A boundary element formulation for a class of non-local damage models. *International Journal of Solids and Structures*, vol. 36, pp. 3617-3638.

Guiggiani, M., & Casalini, P., 1987. Direct computation of Cauchy principal value integrals in advanced boundary elements. *International Journal for Numerical Methods in Engineering*, vol. 24, pp. 1711-1720.

Herding, U., & Kuhn, G., 1996. A field boundary element formulation for damage mechanics. *Engineering Analysis with Boundary Elements*, vol. 18, pp. 137-147.

Huang, Q., & Cruse, T. A., 1993. Some notes on singular integral techniques in boundary element analysis. *International Journal for Numerical Methods in Engineering*, vol. 36, pp. 2643-2659.

Lachat, J. C., & Watson, J. O., 1976. Effective numerical treatment of boundary integral equations - A formulation for three dimensional elastostatics. *International Journal for Numerical Methods in Engineering*, vol. 10, pp. 991-1005-2659.

Lin, F.-B., Yan, G., Bazant, Z. P., & Ding, F., 2002. Non-local strain-softening model of quasi-brittle materials using boundary element method. *Engineering Analysis with Boundary Elements*, vol. 26, pp. 417-424.

Manzoli, O. L., Pedrini, R. A., & Venturini, W. S., 2009. Strong discontinuity analysis in solid mechanics using boundary element method. In Sapountzakis, E. J. & Aliabadi, M. H., eds, *Advances in Boundary Element Techniques X - Proceedings of the 10th International Conference (BETEQ/2009)*, pp. 323-329.

Manzoli, O. L., & Venturini, W. S., 2004. Uma formulação do MEC para a simulação numérica de descontinuidades fortes. *Revista Internacional de Métodos Numéricos para Cálculo y Diseño en Ingeniería*, vol. 20, n. 3, pp. 215-234.

Manzoli, O. L., & Venturini, W. S., 2007. An implicit BEM formulation to model strong discontinuities. *Computational Mechanics*, vol. 40, pp. 901-909.

Mendelson, A., 1973. *Boundary integral methods in elasticity and plasticity*. Tech. rep. NASA TN D-7418, NASA, USA.

Mukherjee, S., 1977. Corrected boundary-integral equations in planar thermoelastoplasticity. *International Journal of Solids and Structures*, vol. 13, pp. 331-335.

Oliver, J., 1996. Modelling strong discontinuities in solid mechanics via strain softening constitutive equations. Part 1: Fundamentals. *International Journal for Numerical Methods in Engineering*, vol. 39, pp. 3575-3600.

Rajgelj, S., Amadio, C., & Nappi, A., 1992. Application of damage mechanics concepts to the boundary element method. In Brebbia, C. A. & Ingber, M. S., eds, *Seventh International Conference on Boundary Element Technology (BETECH/92)*, pp. 617-634.

Riccardella, P. C., 1973. *An implementation of the boundary integral technique for planar problems in elasticity and elastoplasticity*. Tech. rep. SM-73-10, Carnegie Mellon University, Pittsburgh,USA.

Simo, J. C., & Ju, J. W., 1987. Strain- and stress-based continuum damage models - I. Formulation. *International Journal of Solids and Structures*, vol. 23, n. 7, pp. 821-840.

Simo, J. C., Oliver, J., & Armero, F., 1993. An analysis of strong discontinuities induced by strain-softening in rate-independent inelastic solids. *Computational Mechanics*, vol. 12, pp. 277-296.

Sládek, J., Sládek, V., & Bazant, Z. P., 2003. Non-local boundary integral formulation for softening damage. *International Journal for Numerical Methods in Engineering*, vol. 57, pp. 103-116.

Swedlow, J. L., & Cruse, T. A., 1971. Formulation of boundary integral equations for three dimensional elastoplastic flow. *Journal of Solids and Structures*, vol. 7, pp. 1673-1683.

Telles, J. C. F., 1983. *The Boundary Element Method Applied to Inelastic Problems*. Springer-Verlag.

Telles, J. C. F., & Brebbia, C. A., 1979. On the application of the boundary element method to plasticity. *Applied Mathematical Modelling*, vol. 3, n. 4, pp. 466-470.

Telles, J. C. F., & Carrer, J. A. M., 1991. Implicit procedures for the solution of elastoplastic problems by the boundary element method. *Mathematical and Computer Modelling*, vol. 15, pp. 303-311.